

A coupled stress and energy model for mixed-mode cracking of adhesive joints

Philipp Weißgraeber^{1,*}, Wilfried Becker¹

¹ FG Strukturmechanik, TU Darmstadt, Germany

* Corresponding author: weissgraeber@fsm.tu-darmstadt.de

Abstract This work is concerned with the analysis of failure of adhesive joints. Typically adhesive joints fail due to cracking of the adhesive with cracks originating from the reentrant corner of the adherend and the adhesive. A failure model based on a coupled stress and energy criterion settled in the framework of Finite Fracture Mechanics (FFM) is proposed in this work. The main idea of coupled criteria in FFM is that cracks of finite size are predicted when a stress criterion is fulfilled on all points of the considered crack and simultaneously an energy criterion is fulfilled.

A failure model for adhesively bonded single lap joints is worked out that makes use of an extended weak interface model. Its closed-form analytical nature allows for an efficient formulation of the non-linear failure criterion. The effects of the involved geometric parameters are examined in detail. A comparison of the failure load predictions to experimental results is given and shows a good agreement. It is shown that the effect of the adhesive layer thickness is incorporated correctly. The failure model and its implications on the understanding of failure of adhesive joints are discussed in detail.

Keywords Brittle fracture, Finite Fracture Mechanics, adhesive joints

1. Introduction

Adhesive joints can be an interesting alternative joining method. They have several distinctive advantages over other joining techniques as e.g. welding or bolting. Adhesive bonding allows for large surface joining of thin-walled structures that can have dissimilar materials. The resulting joint has a smooth surface and a sealing function is given. But uncertain failure load predictions and lacking knowledge of failure mechanisms still hinder the widespread use of adhesive joints. To make use of their advantageous features a better understanding of this joining method must be achieved. In the last decades many researchers have worked on an improved understanding of adhesive joints. An overview on the performed research can be found in the comprehensive textbooks of this field, e.g. [1,5].

Failure models for adhesive joints mainly make use of three different approaches, namely strength of materials, fracture mechanics and damage mechanics. Most of the works given in literature focus on strength of material approaches as it has the longest history and it is well known. Unfortunately these approaches lack in the correct description of some important features. Various effects of the involved geometric parameters of a simple joint configuration cannot be fully described by these approaches. A typical outcome is for example that the strength of the adhesive seems to depend on certain geometric parameters. No solid physical explanation can be given for such a relation. The aim of the present work is to present a new failure model for adhesive joints that correctly describes the effect of the geometrical parameters and makes accurate predictions for the failure load.

2. Theoretical background

2.1. Coupled stress and energy criterion

In this work a coupled stress and energy criterion [11] is used to predict crack initiation. The criterion requires two basic material parameters: the strength of the material and the fracture toughness. The criterion is settled in the framework of Finite Fracture Mechanics (FFM) [9] that

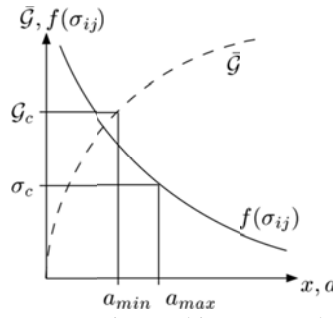


Figure 1. The stress distribution at a stress concentration and incremental energy release rate as a function of the crack length given for a general situation. The upper and lower bounds for the crack length that result from the stress and energy criterion are shown as well.

considers cracks of finite length. This allows for the assessment of crack initiation of uncracked structure, which is a remarkable advantage over classical linear elastic fracture mechanics approaches. Finite cracks have been addressed by several researchers in literature, e.g. [10,12,13,15]. The basic idea of the coupled stress and energy criterion is that the instantaneous formation of a finite crack is predicted when a stress criterion is fulfilled over the full length of the considered crack and the energy balance is fulfilled. The energy balance requires in the style of Griffith's criterion that the energy that is released in the formation of the crack is equal or exceeds the energy that is required to form the crack. Considering a crack of length a and width b with its surface Ω_c the whole coupled criterion can be written as:

$$f(\sigma_{ij}(x_i)) \geq \sigma_c \quad \forall x_i \in \Omega_c \quad \wedge \quad \bar{\mathcal{G}}(a) \geq \mathcal{G}_c \quad (1)$$

The stress criterion f is a function of the stress tensor σ_{ij} and must be chosen appropriately. σ_c is the strength and \mathcal{G}_c is the fracture toughness of the considered material. The quantity $\bar{\mathcal{G}}$ is the so-called incremental energy release rate, which is the averaged energy release rate over the finite crack length:

$$\bar{\mathcal{G}}(a) = \frac{1}{a} \int_0^a \mathcal{G}(\tilde{a}) d\tilde{a}. \quad (2)$$

To assess the minimal load F_f , hence the effective strength, both variables of the criterion have to be identified. Both inequalities are required to identify the finite crack length a and the failure load F_f . In certain cases the stresses and the incremental energy release rate show a monotonic dependence on the crack length and the two inequalities revert to equalities. Such geometries are called positive geometries. In such cases sometimes closed-form solutions for the failure load and the crack length can be given. In the general case of inequalities an optimization problem has to be solved. The lowest load has to be found that satisfies both inequalities for any admissible crack length.

$$F_f = \min_{F,a} \left\{ F \mid f(\sigma_{ij}(x_i)) \geq \sigma_c \quad \forall x_i \in \Omega_c \quad \wedge \quad \bar{\mathcal{G}}(a) \geq \mathcal{G}_c \right\} \quad (3)$$

The ingredients for the optimization problem are illustrated in Fig. 1. In this illustration a_{\min} is the lower bound for the crack length that originates from the energetic condition. The incremental energy release typically increases for larger crack length and this leads to the lower bound for the crack length as function of the given load. The stresses are concentrated, possibly even in form of a stress singularity, and show a declining behavior. Thus, the stress criterion leads to an upper bound a_{\max} for the crack length.

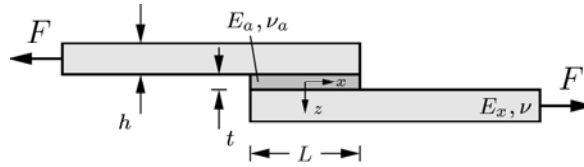


Figure 2. The considered single lap joint configuration

2.2. Linear elasticity solution for the single lap joint

To obtain an efficient failure model a closed-form solution of the mechanical behavior of the single lap joint has been chosen in this work. Since the pioneering works by Volkersen [17] and the work by Goland and Reissner [8] many linear-elasticity solutions for the single lap joint have been developed and proposed in literature. Previous works by the authors [18,19] have shown that the simplified models by Volkersen and Goland-Reissner can be used to study the failure behavior of single lap joints but not all effects are covered to the full extent. In this work an extended weak interface model is used to model the adhesive joint, the model proposed by Ojalvo and Eidinoff [14]. The distinctive feature of this model is an extended consideration of the adhesive layer thickness effect and a linear distribution of the shear stresses in the adhesive layer.

Let us consider a single lap joint under axial loading F as shown in Fig. 2.. The height of the adherends shall be h , the thickness of the adhesive layer t and the length of the overlap shall be L . The width of the joint is denoted as b . Young's modulus of the adherend ist denoted as E_x and Young's modulus of the adhesive as E_a . The respective Poisson's ratios are denoted as ν and ν_a . The shear modulus of the adhesive layer is denoted by G_a . The axial coordinate x runs from the middle of the adhesive layer. Due to the large deformations of the adherends due to bending a non-linear dependence of the bending moment at the end of the overlap to the axial force F is used:

$$M = k(F) \frac{h+t}{2} F \quad (4)$$

with $k(F)$ being the non-linear moment factor. In literature many approaches can be found for defining this moment factor. In this work the moment factor given by Tsai and Morton [16] is used:

$$k = \frac{1}{1 + 2\sqrt{2} \tanh \left(\sqrt{\frac{3(1-\nu^2)}{2}} \frac{L}{2h} \sqrt{\frac{F}{E_x h b}} \right)} \quad (5)$$

The peel stress in the midplane (index 0) of the adhesive layer is obtained as follows [14]:

$$\sigma_0 = \frac{F}{bL} \left(A_1 \sinh \left(\alpha_1 \frac{2x}{L} \right) \sin \left(\alpha_2 \frac{2x}{L} \right) + A_2 \cosh \left(\alpha_1 \frac{2x}{L} \right) \cos \left(\alpha_2 \frac{2x}{L} \right) \right) \quad (6)$$

with

$$\alpha_{1,2} = \sqrt{\pm \frac{3t\lambda^2}{2h} + \frac{1}{2} \sqrt{\frac{3E_a L^4}{2E_x t h^3}}} \quad , \quad \lambda = \sqrt{\frac{G_a L^2}{4E_x t h}} \quad (7)$$

The constants A_1 and A_2 have to be obtained from the following boundary conditions.

$$\frac{L^2}{4} \frac{\partial^3 \sigma_0}{\partial x^3} \Big|_{x=\frac{L}{2}} - 3 \frac{\lambda^2 t}{h} \frac{\partial \sigma_0}{\partial x} \Big|_{x=\frac{L}{2}} = -k \frac{3E_a FL}{E_x t h^2 b} \left(1 + \frac{t}{h} \right) \quad (8)$$

$$\left. \frac{\partial^2 \sigma_0}{\partial x^2} \right|_{x=L/2} = k \frac{6E_a F}{E_x t h^2 b} \left(1 + \frac{t}{h} \right) \quad (9)$$

The shear stress in the adhesive layer can be given as

$$\tau = \tau_0 + \frac{G_a}{E_a} \frac{\partial \sigma_0}{\partial x} z \quad (10)$$

with

$$\tau_0 = \frac{F}{bL\Omega^2} \left(\Omega \zeta \frac{\cosh\left(\frac{\Omega 2x}{L}\right)}{\sinh(\Omega)} + \Omega^2 - \zeta \right), \quad (11)$$

$$\zeta = 2\lambda^2 \left(1 + 3 \left(1 + \frac{t}{h} \right)^2 k \right), \quad \Omega = \lambda \sqrt{2 \left(1 + 3 \left(1 + \frac{t}{h} \right)^2 \right)}. \quad (12)$$

As typical for weak interface models, it is assumed that crack advancement corresponds to a shortening of the overlap length. For the case of cracks emerging from one reentrant corner of the adherends and the adhesive layer the following relationship of the differential energy release rate to the peak stresses at the end of the overlap can be derived from the energy stored in the adhesive layer at the end of the overlap:

$$\mathcal{G} = \frac{1}{2} \frac{t}{G_a} \left(\tau_{0,\max}^2 + \left(\frac{G_a}{E_a} \frac{\partial \sigma_0}{\partial x} \Big|_{x=L/2} \right)^2 \frac{t^2}{12} \right) + \frac{1}{2} \frac{t}{E_a} \sigma_{0,\max}^2 \quad (13)$$

As outlined previously the incremental energy release rate is to be obtained from the differential energy release rate by integration. Of course, it must be considered that the peak stresses change when the overlap length decreases with higher crack lengths.

$$\bar{\mathcal{G}} = \frac{1}{a} \int_0^a (\mathcal{G}(L = L_0 - \tilde{a})) d\tilde{a} \quad (14)$$

This integral cannot be solved in closed-form analytical manner but must be solved with a numerical integration scheme.

3. The optimization problem

As discussed previously it is necessary to solve the optimization problem (3) posed by the coupled stress and energy criterion (1) to identify the failure load of the joint. For the stress function f the maximum principal stress criterion is used in this work. In the case of the presently used simplified model of the single lap joint it reads:

$$f(\sigma_{ij}) = \frac{\sigma_0}{2} + \sqrt{\left(\frac{\sigma_0}{2} \right)^2 + (\tau(z = -t/2))^2} \geq \sigma_c \quad (15)$$

As the incremental energy release rate has to be obtained by numerical integration and the stresses exhibit a non-linear dependence on the acting forces the coupled criterion cannot be solved analytically. The more general approach of solving the optimization problem with the two variables

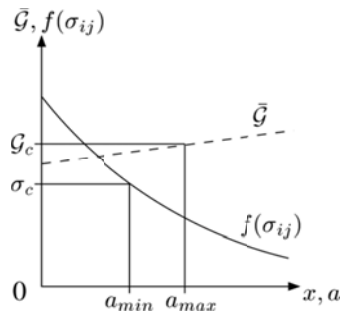


Figure 3. The stress distribution at a stress concentration and incremental energy release rate as a function of the crack length given for the case of the considered weak interface model

failure load and crack length must be followed. The optimization problem can be solved by standard method for restricted optimization. Due to the closed-form nature of the underlying equations an efficient solution is obtained using the Computer Algebra System Mathematica in Version 8.

A closer look at the optimization problem reveals interesting details of the present modeling approach. In Figure 3 the optimization problem is illustrated for the present case of a weak interface model. The most remarkable characteristics are that the stresses and hence the stress criterion do not show a singular behavior, as it is known from linear-elasticity theory and that the incremental energy release rate does not start at zero for vanishing crack lengths as it is expected for the weak singularity of the reentrant corner. The singularity order of the reentrant corner is lower than the well-known crack tip singularity. These deficiencies of the presently used model for the single lap joint concerning the stresses and the energy release rate are well-known and a typical outcome of weak interface models. It will be seen in the following that in the framework of FFM they do not have a strong effect on the results. Figure 3 shows the stress distribution and the incremental energy release rate for a loading that is lower than the failure load. The upper bound for the crack length predicted by the stress criterion is lower than the lower bound for the crack length as predicted by the energy criterion. If the loading is now increased the incremental energy release rate and the stresses will increase as well. With increased energy release and stresses now the upper and lower bound for the finite crack length are approaching each other until they will eventually coincide. Then the lowest load satisfying both conditions of the coupled criterion is found. It is the failure load of the considered joint. It can be seen, that the stress and energy criteria are not evaluated directly at position 0, which is the tip of the reentrant corner. Hence, the previously described deficiencies of the weak interface model do not play a role in the evaluation of the failure load.

4. Results

In this section results of the outlined coupled stress and energy model are presented. The effect of the geometrical parameters of the considered single lap joint on the failure load are pointed out and discussed. Furthermore a comparison to experimental results from literature is shown. In this comparison only material parameters provided from standard tests are used if available to predict the failure load.

4.1. Parameter study

For the parameter study a typical symmetric steel-epoxy joint is considered. Young's moduli of the adherend and the epoxy are: $E_x=210\text{GPa}$, $E_a=3\text{GPa}$. The corresponding Poisson's ratios are

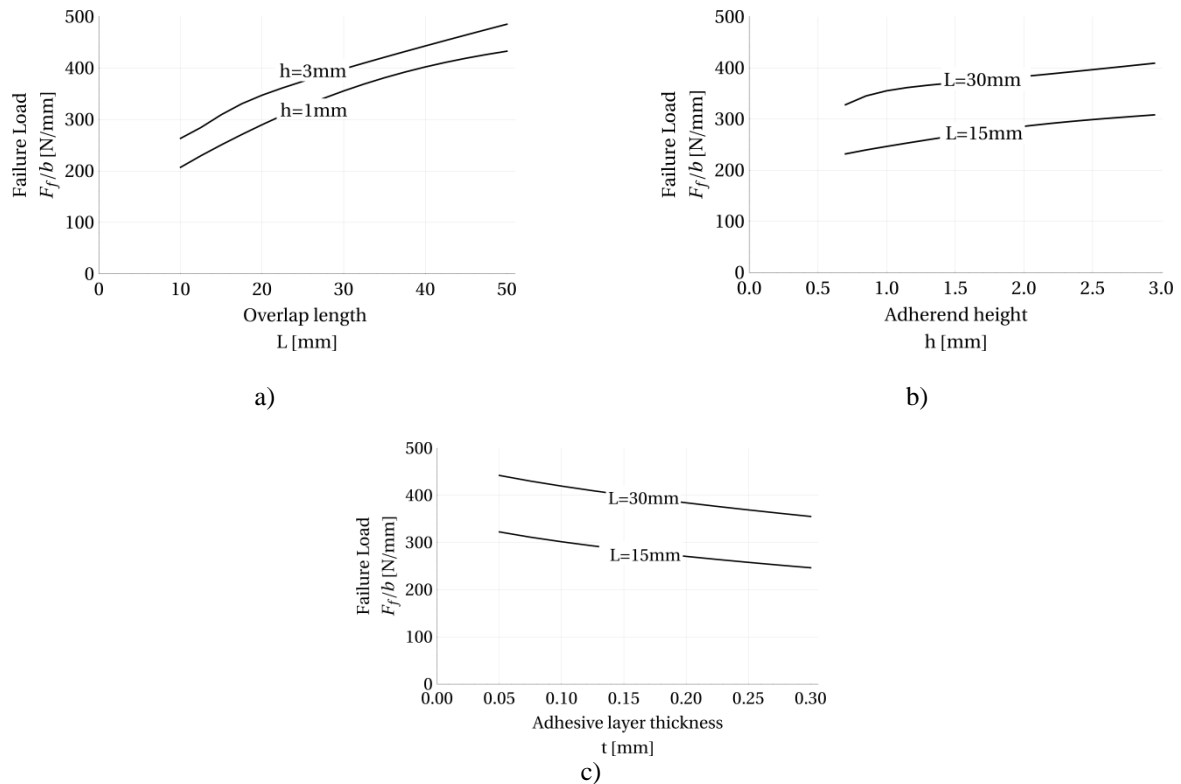


Figure 4. Effect of the geometrical parameters on the failure load of the joint

$\nu=0.3$ and $\nu_a=0.4$. The strength and the fracture toughness are: $\sigma_c = 45\text{MPa}$, $\mathcal{G}_c = .45\text{N/mm}$.

In Fig. 4a the effect of the overlap length L on the failure load is shown. It can be seen, that the failure load increases with higher overlap lengths. As it is well known from experiments a less pronounced increase of the failure load is observed for larger overlap lengths. The basic mechanism is the increased bondline area with more equally distributed stresses. But as the peak stresses at the end of the overlap do not become arbitrarily smaller with larger overlap lengths, the increase is less pronounced for higher overlap lengths. The effect of the adherend height on the failure load is shown in Fig. 4b. An increase of the failure loads is observed with higher adherend heights as it is for larger overlap lengths. The basic mechanism behind this effect is the improved bending stiffness of the adherends. As the bending stiffness increases the peel stresses are distributed more equally. Fig. 4c shows the dependence of the failure load on the adhesive layer thickness. A decrease of the bearable loads is predicted for thicker adhesive layers. This is in very good accordance with knowledge on adhesive joints obtained from practice and experimental results. But it is likewise contrary to failure load predictions from failure models that base on strength of material approaches [6]. The key point is the consideration of energetic criteria. The adhesive layer stores, due its relatively low stiffness, the main part of the elastic strain energy. Hence, it gives the largest contribution to the energy release rate. If now the adhesive layer is increased, the incremental energy release rate increases as well. In this model both criteria, the stress criterion and the energy criterion must be fulfilled simultaneously and hence an increased energy release rate leads to reduced failure loads. This work shows that it is possible to explain the effect of adhesive layer thickness on the failure load by means of a simple linear elastic analysis by consideration of the energy release.

Table 1. Material properties of the adhesives

	E_a [MPa]	ν_a [-]	σ_c [MPa]	\bar{G} [N/mm]	Ref.
AV138/HV998	4890	0.35	39.5	0.38	[2]
Hysol EA 9321	3870	0.36	46.0	0.45	[7]
Redux 326	4440	0.35	50.9	(0.3)	[6]

4.2. Comparison to experimental results

Several experimental studies have been selected for comparison to the failure load predictions. The experimental studies were chosen such that only well documented and repeated studies are used. Only adhesives with substantially brittle behavior were used for the comparison.

The effect of the adhesive layer thickness was studied experimentally by Castagnetti et al. [3] for steel adherends with two different adhesives. The results of the sufficiently brittle adhesive Hysol EA 9514 are used for comparison. In the work by da Silva et al. from 2004 [4] the effect of the overlap length on the failure load of the steel joints with a bismaleimide adhesive Redux 326 was studied. In the study by da Silva et al. from 2006 [7] three different adhesives were tested with steel adherends. From these adhesives two adhesives, AV138 and Hysol EA 9321, were sufficiently brittle. The material data that were used are summarized in Table 1. The strength and the fracture toughness are not identified by means of the used experimental results. Material parameters from standard tests that are given in literature [2,6,7] are used. No specific value for the fracture toughness could be found in literature for the bismaleimide adhesive Redux 326. It is assumed that the fracture toughness attains values around 0.3 N/mm.

The comparisons of the present failure model to the experimental results are shown in Fig. 5a-5c. Obviously, the failure load predictions agree well with the experimental results. Especially when the scattering of the experimental results is considered it becomes clear that the failure load prediction by the present model is of good quality. Another important feature is that the effects of the geometrical parameters are covered correctly by the present model. Especially the adhesive layer thickness effect has been subject to many studies that try to explain the effect on the failure load. If only stress criteria are used it appears that the strength of the adhesive reduces if thinner bondlines are considered. No physically sound explanation can be given for such a change of the adhesive strength. The present model can correctly predict the effect of the adhesive layer thickness by an additional energetic condition that must be satisfied simultaneously.

5. Summary

A new failure model for adhesive joints has been given. It bases on a coupled stress and energy criterion in the framework of FFM. A closed-form analytical model for the mechanical behavior of a single lap joint is used to set up the failure model. The failure model requires two basic failure parameters, the strength and the fracture toughness of the adhesive. A study of the effect of the geometrical parameters on the failure load on adhesive joints is shown and discussed. The predicted effects are in good accordance to general knowledge on adhesive joints. Furthermore a comparison to experimental results is shown. In general it shows a good accordance of the prediction and the experimental results. All trends are covered very well. Only failure parameters as given in published results from standard tests are used in the comparison and no fitting of the input parameters needs to be performed. A remarkable outcome is the fact that the effect of the adhesive layer thickness is covered correctly.

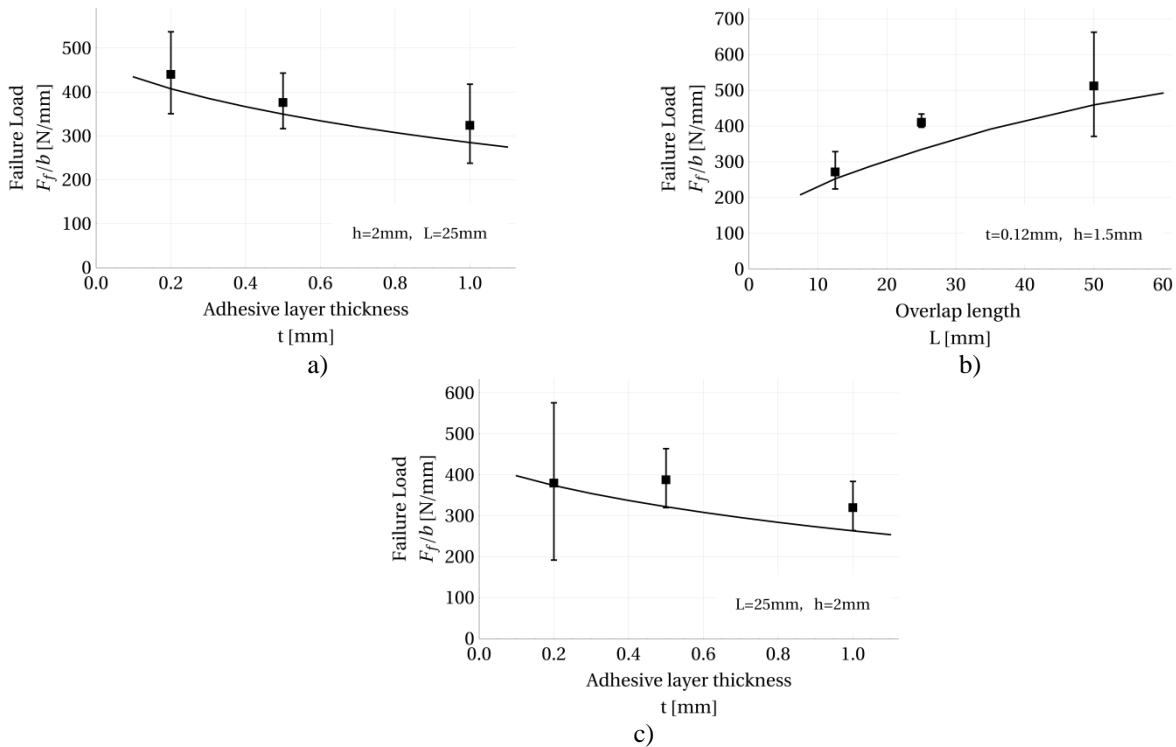


Figure 5. Comparison to experimental results

References

- [1] Adams R, Comyn J, and Wake W. Structural adhesive joints in engineering. Springer, 1997.
- [2] Campilho R, Banea M, Pinto A, da Silva L, and De Jesus A. Int J Adhes Adhes, 2011.
- [3] Castagnetti D, Spaggiari A, and Dragoni E. J Adhes, 87(7-8):780, 2011.
- [4] da Silva L, Adams R, and Gibbs M. Int J Adhes Adhes, 24(1):69, 2004.
- [5] da Silva L and Campilho R. Advances in Numerical Modeling of Adhesive Joints. Springer, 2011.
- [6] da Silva L, das Neves P, Adams R, Wang A, and Spelt J. Int J Adhes Adhes, 29(3):331, 2009.
- [7] da Silva L, Rodrigues T, Figueiredo M, Moura MD, and Chousal J. J Adhes, 82(11):1091, 2006.
- [8] Goland M and Reissner E. J Appl Mech, 11(1):A17, 1944.
- [9] Hashin Z. J Mech Phys Solids, 44(7):1129, 1996.
- [10] Hebel J, Dieringer R, and Becker W. Eng Fract Mech, 77(18):3558, 2010.
- [11] Leguillon D. Eur J Mech A-solid, 21(1):61, 2002.
- [12] Mantić V. Internat J Solids Structures, 46(6):1287, 2009.
- [13] Martin E, Leguillon D, and Carrère N. Internat J Solids Structures, 47(9):1297, 2010.
- [14] Ojalvo I and Eidinoff H. Aiaa J, 16(3):204, 1978.
- [15] Tran V, Leguillon D, Krishnan A, and Xu L. Int J Fracture, 35(1):1, 2012.
- [16] Tsai M and Morton J. J Appl Mech, 61(3):712, 1994.
- [17] Volkersen O. Luftfahrtforschung, 15(1/2):41, 1938.
- [18] Weißgraeber P and Becker W. Key Eng Mater, 471:1075, 2011.
- [19] Weißgraeber P and Becker W. In Proceedings of the 32nd Risø International Symposium in Materials Science, 479–486, 2011.